

A Note on the Correlation between b-value and Fractal Dimension from Synthetic Seismicity

JEEN-HWA WANG*

(Received 21 June 1991; Revised 30 December 1991)

ABSTRACT

Seismicity is dynamically simulated by one-dimensional mass-spring model with fractal distribution of breaking strengths. A linearly rapidly-weakening-and-hardening friction law controls the sliding of the mass. The frequency-magnitude relations from synthetic seismicity for five values of fractal dimension show that b-values for events with intermediate magnitudes are close to 1, while those for events with larger magnitudes are from 1.68 to 2.52. For small events, the $\log N$ values are almost constant.

1. INTRODUCTION

Gutenberg and Richter (1955) first mentioned the linear law between $\log N$ and M , where M is the earthquake magnitude and N is the cumulative frequency of earthquakes with magnitude greater than M , in the following form: $\log N = a - bM$. The b-value varies from region to region and is also dependent upon the used period of time, but is generally in the range of from 0.8 to 1.2. The variation of b-value before and after a major earthquake has been as an earthquake precursor (Smith, 1986; Chen *et al.*, 1990). The b-value is also correlated to geotectonics (Wang, 1988; Tsapanos, 1990). An understanding of physical basis of b-value would be significant to the studies on earthquake generation process and earthquake prediction.

Earlier studies on the physical processes associated b-value were primarily based on laboratory work of rock fracture. Mogi (1967) reported the effect of degree of heterogeneity of the media on b-value. Schulz (1968) correlated the increase of b-value with the decrease of the ambient stress level. Recently, numerous theoretical studies have been done to explore the relation of b-value with fault structure and fault dynamics. The studies are based on several aspects of physics: 1. fragmentation of materials (Turcotte, 1986a); 2. fractal distribution of strain and stress of crustal deformation (Turcotte, 1986b); 3. percolation

* *Institute of Earth Sciences, Academia Sinica, Taipei, Taiwan, R. O. C.*

theory (Lomnitz-Adler, 1988); 4. cellular automata with self-organization criticality (Bak and Tang, 1989; Ito and Matsuzaki, 1990; Nakanishi, 1990; Brown *et al.*, 1991); and 5. dynamic simulation (Carlson and Langer, 1989; Wang and Knopoff, 1991). The b-value obtained by Brown *et al.* (1991) is 1.5, while those done by others are about 1.

The fault zones where earthquakes occur are quite complex. Map and field observations (Aviles *et al.*, 1987; Okubo and Aki, 1987) and laboratory observations (Brown and Scholz, 1985; Power *et al.*, 1987) showed fractal distribution of fault surface. The fractal dimension, whose explanation can be found in Turcotte (1986a), describes quantitatively the scale invariance of a structure or provides a measure of the relative importance of large versus small objects. Hence, fractal dimension might be a factor to influence b-value. The correlation between b-value and fractal dimension (D) is described by $b = D/3$ in Turcotte (1986a) and by $b = D/2$ in Turcotte (1986b). From a probabilistic synthesis, Aki (1981) speculated the relation of the two parameters to be $b = D/2$. However, from the analysis of the actual earthquake data in the Tohoku area, Hirata (1989) reported a negative correlation ($D = 2.3 - 0.73 b$) between the two parameters. The ranges of D values and b-values are from 1.3 to 1.8 and from 0.7 to 1.2, respectively. It is obvious that more studies are needed to explore the relation between the two parameters. Wang and Knopoff (1991) used an one-dimensional mass-spring model (Burrige and Knopoff, 1967) with fractal distribution of breaking strengths for the simulation of seismicity. Here, an attempt is to study the possible correlation between b-value and fractal dimension from synthetic seismicity.

2. THEORY

The one-dimensional mass-spring model consists of a chain of N masses with equal mass (m) and springs with each mass being linked by a spring of strength (K) with two other neighbors. Each mass is also pulled through a spring of strength (L) by a constant velocity (v). Each mass is located at position x_j , measured from its initial equilibrium position. This system is illustrated schematically in Figure 1. Each mass is subjected to a velocity-dependent friction law, $F(\dot{x}_j)$, where \dot{x}_j is the velocity of the j -th mass. Hence, the equations of motion for the system are:

$$m \ddot{x}_j = K(x_{j+1} - 2x_j + x_{j-1}) - L(x_j - vt) - F(\dot{x}_j). \quad (1)$$

The dots represent differentiation with respect to time t . It is noted that memory effect is not included. The periodic boundary condition is applied at the two end masses.

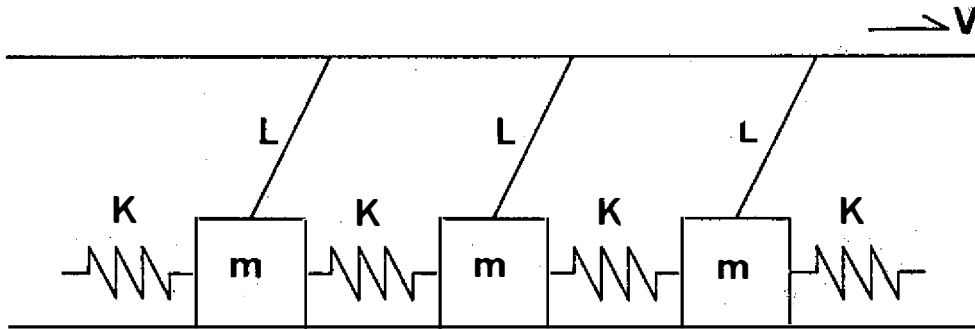


Fig. 1. One-dimensional mass-spring model.

As one mass starts to slide, the static friction force subjected to this mass immediately becomes the dynamic one, which is time-dependent (Dieterich, 1978). The velocity-dependent friction law is very commonly considered for controlling sliding of the fault (Ruina, 1983). Dieterich (1978), Ruina (1980), Tullis and Weeks (1986) and some others showed that at low velocities, the friction decreases with increasing velocity (i.e. velocity-weakening). However, Weeks and Tullis (1985), Shimamoto (1986), and Blanpied *et al.* (1987) reported that the velocity dependence actually changes from negative to positive (i.e. velocity-hardening) as slip velocity is increased. Horowitz (1988) suggested a mixed state variable friction law to describe both velocity-dependent weakening and hardening processes. Hence, a velocity-dependent friction law, including velocity-weakening process as the sliding velocity smaller than a critical velocity (v_c) and velocity-hardening process as sliding velocity greater than v_c , is taken into account. The critical velocity is the one at which the dynamic friction force reaches the minimum value. The generalized velocity-dependent friction law is quite complicated. In this study, a linear friction law, including a decreasing function for weakening process and an increasing function for hardening process (see Figure 2):

$$F(\dot{x}_j) = F_{o_j} - \gamma_1 \dot{x}_j \quad (\dot{x}_j \leq v_c); \tag{2a}$$

$$= q F_{o_j} + \gamma_2 \dot{x}_j \quad (\dot{x}_j > v_c) \tag{2b}$$

is taken as the first-order approximation of the friction law. The decreasing rate (γ_1) and increasing rate (γ_2) for the variation of friction force with sliding velocity are two parameters of the model. At velocity v_c , the dynamic friction force is the minimum value ($q F_o$), where q is a positive number smaller than 1.

The distribution of breaking strengths or static friction forces at all masses of the system is considered to be fractal. The Midpoint Displacement Method developed by Saupe (1988) is used to yield fractal distribution. This method

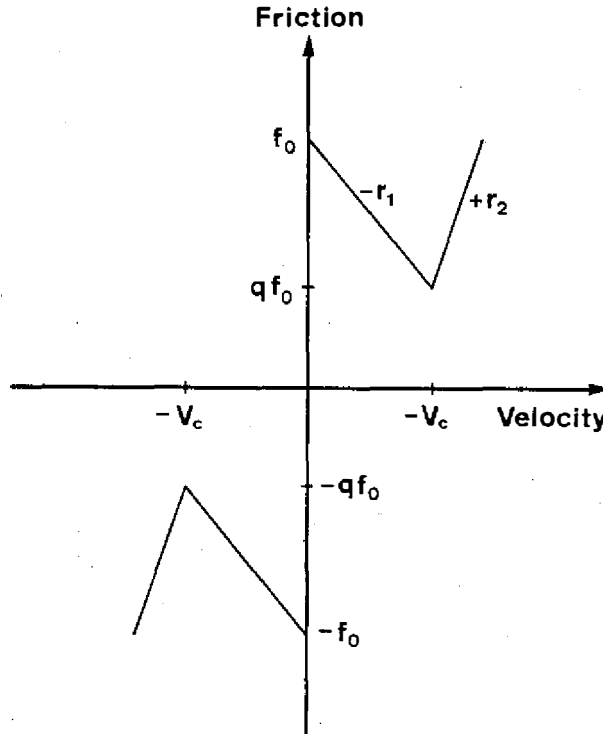


Fig. 2. Linearly velocity-dependent friction law. Quantities f_0 and v_c are breaking strength and critical velocity, respectively.

can only produce fractals at $N (= 2^{\text{level}} + 1)$ points, where “level” is a positive integer. The normalized fractal distributions of breaking strengths for five values of fractal dimension: 1.1, 1.3, 1.5, 1.7, and 1.9 are shown in Figure 3. Besides, a parameter defined as the ratio of the difference of the maximum and minimum values of breaking strengths to the mean value of them is taken into account to control the roughness of the fault. This parameter is named as roughness (R). In Figure 3, the R value is 0.5 for the five distributions.

In the practical computation, Equation (1) is normalized by letting m and L be one unit. Hence, Equation (1) becomes

$$\ddot{x}_j = s(x_{j+1} - 2x_j + x_{j-1}) - x_j + vt - f_j(\dot{x}_j) \tag{3}$$

where $s = K/L = K$. From the observed data, v is about 50 mm/yr, or the order of 10^{-12} km/yr.

For solving this problem with nonlinear boundary condition, a technique developed by Wilson and Clough (1962) is used to numerically integrate Equation (1). The velocities $\dot{x}_i(t + \delta t)$ and displacements $x_i(t + \delta t)$ at times $t + \delta t$ for the i -th sliding mass can be calculated by the following expressions:

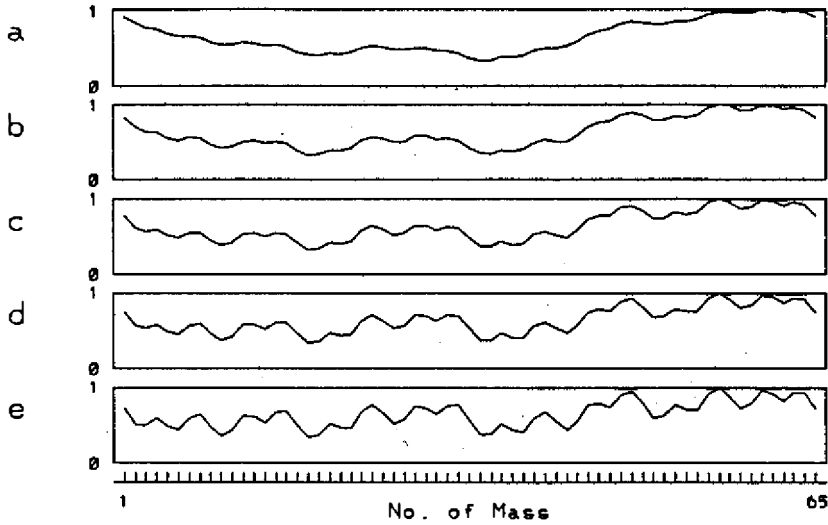


Fig. 3. Normalised fractal distribution of breaking strengths: (a) for $D=1.1$, (b) for $D=1.3$, (c) for $D=1.5$, (d) for $D=1.7$ and (e) for $D=1.9$.

$$\dot{x}_i(t + \delta t) = \dot{x}_j(t) + \left(\frac{\delta t}{2}\right)\ddot{x}_i(t) + \left(\frac{\delta t}{2}\right)\ddot{x}_i(t + \delta t) \tag{4a}$$

and

$$x_i(t + \delta t) = x_i(t) + \delta t \dot{x}_i(t) + \left(\frac{\delta t^2}{3}\right)\ddot{x}_i(t) + \left(\frac{\delta t^2}{6}\right)\ddot{x}_i(t + \delta t) \tag{4b}$$

where $\ddot{x}_i(t)$ is the acceleration of the i -th mass at time t .

For a certain mass point, as the sum of tectonic driving force and spring forces from its neighbors exceeds frictional force, this mass point is accelerated and starts to slide. After a while, the increase of either spring forces due to the change of relative positions of the mass and its neighbors or dynamic friction force as the sliding velocity is greater than v_c gives rise to resistant force to decelerate the sliding mass. The mass stops and sticks when the total force acting on the mass becomes zero. The increase of total force due to the increase of tectonic driving force will reactivate the mass.

The displacement of a mass is measured from its new equilibrium position to the position where it sticks. The position where the mass sticks after motion is a new equilibrium position for the next stage of motion. Since several neighboring masses slide almost simultaneously during a certain time interval, the time history of sum of displacements of such masses is taken to represent one event. Seismic energy released by one mass for an event equals to the product of its maximum displacement and stress drop. The logarithmic value of the sum

of seismic energy of all masses for an event is considered to be the magnitude (M) of the event.

3. NUMERICAL RESULTS AND DISCUSSION

The tectonic driving force due to the moving plate with velocity v is a main source to push the mass to slide. From the real data, v is a very small value of the order of 10^{-12} units, hence, a very long computational time is needed for yielding significant pattern of synthetic seismicity. In this work, a larger v value of 10^{-4} units is used. The time unit δt is 0.1, which is much smaller than natural period of 2π of the oscillation of one mass. For the frictional law, only the case with $\gamma_1 = -\infty$ and $\gamma_2 = +1$ and $q = 0.8$ is considered. Wang and Knopoff (1992) study the effects due to the variation of the parameters of frictional law on synthetic seismicity in detail. Their major results are: (1) Both γ_1 and γ_2 values influence the b-value (2) Smaller q value gives smaller b-value; and (3) Larger value of stiffness (s) produces smaller b-value. Stiffness is a factor to represent the coupling between the moving plate and masses. In this study, the s value is taken to be 10. Roughness (R) is also a significant factor to change synthetic seismicity pattern and b-value. Practical computation shows that small R value, for instance 0.1, will cause a large number of masses to slide, thus producing large events. For understanding the distribution of events magnitudes, a larger R value of 0.5 is selected.

Figure 4 shows an example of the spatial-temporal pattern (ST-pattern) with $D = 1.5$. Each line segment represents one event. The spatial distribution of breaking strengths for all masses is shown by symbols '+'. The amount of breaking strength increases from left to right. The maximum and minimum values of breaking strengths are 5.00 and 1.67 units. Longer line segment of the ST-pattern indicates larger number of broken masses and thicker line segment represents longer sliding time of the related masses. It can be seen that in the time interval earlier than $t_c = 2 \times 10^6$ units, larger events repeatedly appear at the masses with higher breaking strength in the lower part of the fault. This phenomenon does not appear after time t_c . Besides, the time intervals of occurrence of events are smaller before than after t_c . It is assumed that the computed events in the time interval before t_c are the unsteady- or transient-state solutions. Hence those events will not be included in the further discussion. The time series of number of events for the five values of fractal dimension are shown in Figure 5. It is noted that those time series are different for various values of fractal dimension. However, the detailed analysis of the ST-pattern and the related time series will be given in a separate paper. Here only the slope of data points of $\log N$ vs. M is taken into account.

The data points of $\log N$ vs. M for the five time sequences of synthetic

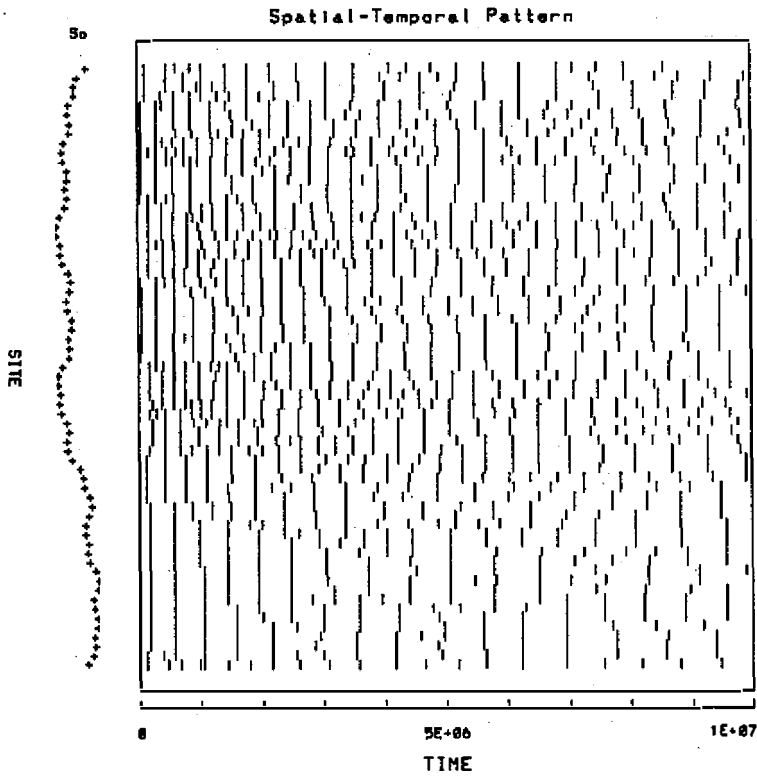


Fig. 4. Spatial-temporal pattern of events for $D=1.5$.

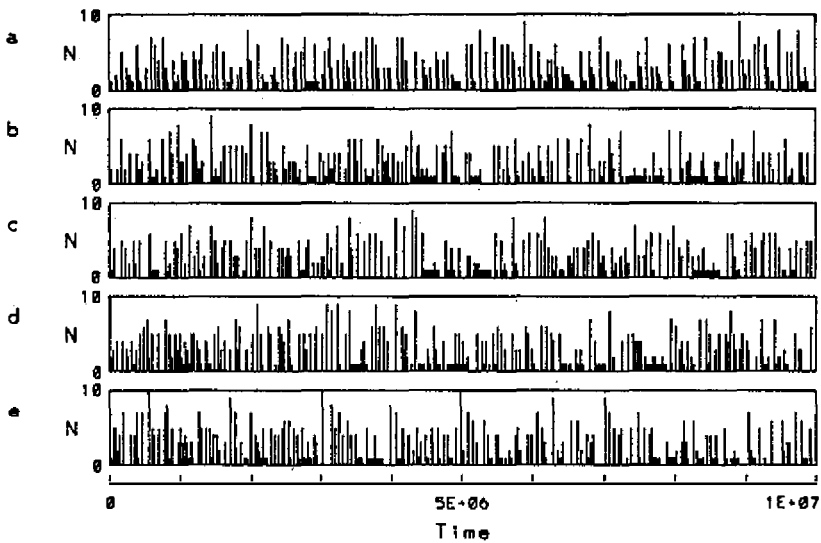


Fig. 5. Time series of number of events: (a) for $D=1.1$, (b) for $D=1.3$, (c) for $D=1.5$, (d) for $D=1.7$ and (e) for $D=1.9$.

seismicity are shown in Figure 6. The pattern of data points seems to be similar to that obtained from the real earthquake data. For the five cases, the distributions of data points can be divided into three portions. The first portion has data points with magnitudes smaller than -0.6 and the related $\log N$ values are nearly constant. The second portion includes the data points with magnitudes ranging from -0.6 to $+0.1$. The data points distribute almost around a line with slope of -1 . The third portion includes the data points with larger magnitudes and the related $\log N$ values decrease rapidly with magnitude. For the first and second portions, the data points of the five values of fractal dimension have very similar distribution, but for the third one, the data points are somewhat scattering. It is obvious that the data points of the second portion seem to follow a linear relation as suggested by Gutenberg and Richter (1953). Due to normalization of the problem and definition of magnitude in this study, the present magnitude is not equal to the commonly-used earthquake magnitude, and the slope of linear portion of data points is not exactly the b-value of Gutenberg and Richter's relation. Nevertheless, this slope is to some degree similar to the b-value because both of them show the correlation between frequency and size of earthquakes. The slope obtained from synthetic seismicity would provide significant information for understanding the physics of the b-value. For convenience, the present slope is called as b-value.

The b-values together with standard deviation and magnitude ranges for the second and third linear portions (denoted by SLP and TLP respectively)

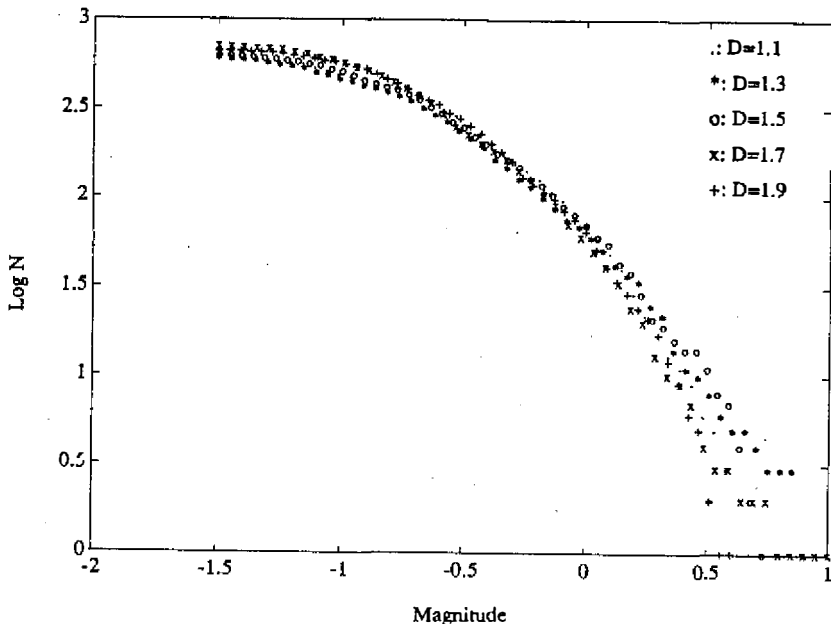


Fig. 6. Figure shows the data points of $\log N$ vs. M for five values of fractal dimension.

for the five values of fractal dimension are shown in Table 1. For the purpose of reference, included also in the table are the magnitude ranges and numbers of events. The numbers of events for all cases are greater than 610. The magnitude ranges are essentially the same for the five cases. The values of standard deviation vary from 0.01 to 0.04 for SLP and from 0.06 to 0.15 for TLP. Obviously, the b -values of TLP are larger than those of SLP. The b -value of $D = 1.5$ is the smallest value among the five values. The b -values of $D \leq 1.5$ are very close to 1; while those of $D > 1.5$ deviate from 1.

As the above mention, the liner relations between b and D values are given by several authors. However, the b -values obtained from the present work are close to 1 and not remarkably dependent upon D values. A possible reason for this difference is that the D value used by those authers is related to the geometry of the fault, while the D value used in this work is concerning the distribution of breaking strengths of the fault.

Comparison of Figures 3 and 4 shows that the time series of five values of fractal dimension are different in spite of the similarity of their b -values. It indicates that the ST-pattern of synthetic seismicity is more sensitive to the variation of fractal dimension than the b -value. The linear frequency-magnitude relation is considered to be a universal or collective trail of seismicity (Keilis-Borok, 1990). The present model is a complicated one consisting of many simple systems with masses and springs, which obey simple physical laws. However, the whole system is self-organized to show an integral trait, which is very independent upon the details of the properties of its elements (Kadanoff, 1991). The b -value is such a parameter to indicated the integral trait of the fault system.

Lomnitz-Adler (1985), Carlson and Langer (1989) and Nakanishi (1990) reported the existence of events ruptured at all masses. Such events have largest values of magnitude and their $\log N$ values can not be predicted from the linear equation obtained from the smaller events. Those events are called as "runaway events" by Knopoff (1990), who correlated them either with the finite size of the

Table 1. Table shows the numbers of events (N), magnitude ranges for the whole data points (WMR), magnitude ranges for linear portion of data points of $\log N$ vs. M (LMR) and b -values with their standard errors, far the second (SLP) and third (TLP) linear portions for five fractal dimensions (D).

D	N	SLP	TLP
1.1	627	1.16±0.02	2.40±0.09
1.3	610	1.13±0.01	1.81±0.06
1.5	630	1.08±0.02	1.68±0.08
1.7	708	1.26±0.04	2.18±0.09
1.9	666	1.30±0.04	2.52±0.15

lattice used in the computations or with the correlations across the fracture. These authors used homogeneous models for breaking strengths. For those models, there is a characteristic length above which the stress concentration is always larger than the breaking strength. However, no such a runaway event can be found from the real data and from the present computational results. The use of homogeneous model for the synthesis of seismicity is considered to be not appropriate.

4. CONCLUSIONS

The b-values for events with intermediate magnitudes obtained from synthetic seismicity by one-dimensional mass-spring models with fractal distributions of breaking strengths are close to 1. But those for events with larger values of magnitude are from 1.68 to 2.52. For small events, the $\log N$ values are almost zero.

Acknowledgements. This work was completed when the author visited the Institute of Geophysics and Planetary Physics, University of California at Los Angeles. He sincerely thanks the Seismology Group of the Institute for using computing facilities. Numerous beneficial suggestions and comments from Prof. L. Knopoff are acknowledged. The author was financially supported by the National Sciences Council, ROC, through Oversea Research Program.

REFERENCES

- Aki, K., 1982: A probabilistic synthesis of precursor phenomena, In: *Earthquake Prediction*, ed. by D. W. Simpson and P. G. Richards, AGU, Washington D. C., 556-574.
- Aviles, C. A., C. H. Scholz and J. Boatwright, 1987: Fractal analysis applied to characteristic segments of the San Andreas fault, *J. Geophys. Res.*, **92**, 331-344.
- Bak, P. and C. Tang, 1989: Earthquakes as a self-organized critical phenomenon, *J. Geophys. Res.*, **94**, 15635-15637.
- Blanpied, M. L., T. E. Tullis, and J. D. Weeks, 1987: Frictional behavior of granite at low and high sliding velocities, *Geophys. Res. Lett.*, **14**, 554-557.
- Brown, S. R. and C. H. Scholz, 1985: Broadbandwidth study of the topography of natural rock surfaces, *J. Geophys. Res.*, **90**, 12575-12582.
- Brown, S. R., C. H. Scholz, and J. B. Rundle, 1991: A simplified spring-block model of earthquakes, *Geophys. Res. Lett.*, **18**, 215-218.
- Burridge, R. and L. Knopoff, 1967: Model and theoretical seismicity, *Bull. Seism. Soc. Am.*, **57**, 341-371.
- Carlson, J. and J. S. Langer, 1989: Mechanical model of an earthquake fault, *Phys. Rev. A*, **40**, 6470-6484.
- Chen, K. C., J. H. Wang, and Y. L. Yeh, 1990: Premonitory phenomena of the May 10, 1983 Taipingshan, Taiwan earthquake, *TAO*, **1**, 1-21.
- Dieterich, J. H., 1978: Time-dependent friction and the mechanics of stick slip, *Pure Appl. Geophys.*, **116**, 790-806.

- Gutenberg, B. and C. F. Richter, 1955: Frequency of earthquakes in California, *Bull. Seism. Soc. Am.*, **34**, 185-18.
- Hirata, T., 1989: A correlation between the b-value and the fractal dimension of earthquakes, *J. Geophys. Res.*, **94**, 7507-7514.
- Horowitz, F. G., 1988: Mixed state variable friction laws: some implications for experiments and a stability analysis, *Geophys. Res. Lett.*, **15**, 1243-1246.
- Ito, K. and M. Matsusaki, 1990: Earthquakes as self-organized critical phenomena, *J. Geophys. Res.*, **95**, 6853-6860.
- Kadanoff, L. P., 1991: Complex structures from simple systems, *Phys. Today*, Vol. 44, No. 3, 9-11.
- Keilis-Borok, V. I., 1991: The lithosphere of the earth as a nonlinear system with implications for earthquake prediction, *Rev. Geophys.*, **28**, 19-34.
- Knopoff, L., 1990: The relation between small and large earthquakes, *Extended Abstract, Intern. Symp. on Earthq. Source Phys. and Earthq. Pred.*, Tokyo Univ., Tokyo, Japan, 111-115.
- Lomnitz-Adler, J., 1985: On the magnitude-frequency relation of asperity models, *Tectonophys.*, **120**, 133-140.
- Nakanishi, H., 1990: Cellular-automaton model of earthquakes with deterministic dynamics, *Phys. Rev. A*, **41**, 7086-7089.
- Okubo, P. G. and K. Aki, 1987: Fractal geometry in the San Andreas fault system, *J. Geophys. Res.*, **92**, 345-355.
- Power, W. L., T. E. Tullis, S. R. Brown, G. N. Boitnott and C. H. Scholz, 1987: Roughness of natural fault surface, *Geophys. Res. Lett.*, **14**, 29-32.
- Ruina, A. L., 1980: Friction laws and instabilities: a quasistatic analysis of some dry frictional behavior, Ph. D. thesis, Brown Univ., Providence, R. I.
- Ruina, A. L., 1983: Slip instability and state variable friction laws, *J. Geophys. Res.*, **88**, 10359-10370.
- Saupe, D., 1988: Algorithms for random fractals, Chapter 2, in *The Science of Fractal Images* ed. by H. O. Peitgen and D. Saupe, Springer Verlag, New York.
- Scholz, C. H., 1968: The frequency-magnitude relation of microfracturing in rock and its relation to earthquakes, *Bull. Seism. Soc. Am.*, **58**, 399-415.
- Shimamoto, T., 1986: Transition between frictional slip and ductile flow for halite shear zones at room temperature, *Science*, **231**, 711-714.
- Smith, W. D., 1986: Evidence for precursory changes in the frequency-magnitude b-value, *Geophys. J. R. Astro. Soc.*, **86**, 815-838.
- Tsapanos, T. M., 1990: b-values of two tectonic parts in the Circum-Pacific belt, *Pure Appl. Geophys.*, **134**, 229-242.
- Tullis, T. E. and J. W. Weeks, 1986: Constitutive behavior and stability of frictional sliding of granite, *Pure Appl. Geophys.*, **124**, 383-414.
- Turcotte, D. L., 1986a: Fractals and fragmentation, *J. Geophys. Res.* **91**, 1921-1926.
- Turcotte, D. L., 1986b: A fractal model for crustal deformation, *Tectonophys.*, **132**, 261-269.
- Wang, J. H., 1988: b-value of shallow Taiwan earthquakes, *Bull. Seism. Soc. Am.*, **78**, 1243-1254.
- Wang, J. H. and L. Knopoff, 1991: Dynamic simulation of seismicity by one-dimensional mass-spring model with fractal breaking strength (Abst.) *EOS Trans Suppl.*, AGU, April, 279.

- Wang, J. H. and L. Knopoff, 1992: Velocity-dependent friction law as a factor for controlling seismicity (to be submitted).
- Weeks, J. D. and T. E. Tullis, 1985: Frictional sliding of dolomite: a variation in constitutive behavior, *J. Geophys. Res.*, **90**, 7821-7826.
- Wilson, E. L. and R. W. Clough, 1962: Dynamic response by step-by-step matrix analysis. In *Symposium on the Use of Computers in Civil Engineering*, Lisbon, paper **45**, 1-14.

由合成地震活動研究 b 值和碎形度 之相關性

王錦華

中央研究院地球科學研究所

摘要

利用一維的質點－彈簧模型並配合碎形分佈的破壞強度，以研究地震活動。線性的快減弱－加強型摩擦定理用於控制質點的滑動。由五個碎形度的合成地震活動所得的地震次數－規模關係式顯示：中規模範圍之地震的 b 值接近於 1；而較大規模之地震的 b 值約在 1.68 到 2.52 間。對小地震而言， $\log N$ 值差不多是常數。

